Int. J. Heat Mass Transfer. Vol. 35, No. 10, pp. 2413–2420, 1992
Printed in Great Britain

0017 9310/92 $5.00 + 0.00

Boundary effect on the Bénard–Marangoni instability

H. Q. YANG
CFD Research Corporation, 3325-D Triana Boulevard, Huntsville, AL 35805, U.S.A.

(*Received* 26 *June* 1991 *and in final form* 15 *October* 1991)

Abstract—The conjugate onset instability of a liquid layer with free upper surface and heated from below by a heating coil through a solid plate is studied. The focus is on the effect of the solid plate thickness and its conductivity. It is found that the solid plate with a higher thermal conductivity tends to stabilize the system. In real experiments, it is much more difficult to achieve a perfectly insulating boundary condition than to achieve a perfectly conducting condition for a thermal disturbance. The parallel flow assumption is shown to be valid when the plate thickness and its thermal conductivity are small.

INTRODUCTION

A LIQUID fluid layer with free upper surface and heated from below is subjected to two instability mechanisms. The first one is related to the gravitational force caused by vertical density stratification and is referred to as Rayleigh–Bénard instability. The second one is due to the local variation of interfacial tension and is referred to as Marangoni instability. The Bénard–Marangoni instability has received much attention in both experiments and theoretical studies because scientifically and technologically significant results are expected from low-gravity melt processing and crystal growth processing in an orbiting space craft. Metal melting experiments in SKYLAB gave evidence of surface-tension-driven cellular convection, and it is generally well established that the Bénard–Marangoni effect is responsible for triggering steady and time-dependent flows in crystal growth with free surface. It is also expected that pure crystals can be provided in a reduced gravity environment. The other applications of Bénard–Marangoni convection can be found in oil extraction from porous media, energy storage in molten salts, and chemical engineering of paints, colloids and detergents.

The early study accounting for both buoyancy and surface tension effects on a fluid layer was carried out by Nield [1]. He found that at the onset of convection the driving force for the motion is approximately equal to the sum of the surface and buoyancy forces in the layer. Davis and Homsy [2] studied the role of interfacial deformation in the stability of a horizontal layer heated from below and open to the ambient air (the Nield model). They found that a deformable interface leads to a stabilization relative to the case of a planar interface when the Marangoni number is less than a critical value. The Bénard–Marangoni instability in a system of two fluid layers, where the upper air layer is constrained, has also been studied [3–5]. An excellent review on the subject of thermocapillary instability is consolidated by Davis [6].

In all the past analyses on the Bénard–Marangoni instability, the conditions at the bottom surface are described either as uniform temperature or as uniform heat flux. In the real experiments, such as the one shown in Fig. 1 [3, 4], the liquid layer is supported by a solid plate, which is in turn heated by a heating coil with a constant heat flux. One may expect that if the plate is very thin, the liquid layer is subjected to a uniform heat flux. When the thermal conductivity of the plate is very high, a uniform temperature condition is realized. For the moderate thickness and moderate thermal conductivity of the plate, a Neumann type of condition of the form

$$\nabla Tn = BiT \tag{1}$$

may well represent the general situation. Here Bi is the Biot number. It is important, however, to note that with the consideration of heat conduction in the solid plate, the equivalent Biot number for equation (1) is a strong function of wavenumber of a disturbance. As a result, the instability character deviates from those analyzed previously.

Nield [7] was the first to consider the effect of a finite conductivity slab on a Rayleigh–Bénard system. He studied the condition when the solid slab is located on the upper surface of the liquid layer while the bottom of the surface is at a constant temperature. He expanded the normal functions in a set of orthogonal functions. Lienhard [8] made the analysis procedure systematic. The thickness of the solid plate in his case is infinitely large, so that the resulting Biot number, expressed in the above form, is only dependent on the thermal conductivity ratio of the liquid to the solid and the wavenumber. His tabular data indicates that the critical Rayleigh number for a two-layer system decreases with the increase of fluid layer to outer wall conductivity ratio.

The present study aims at revealing the effect of a solid plate on the Bénard–Marangoni instability of a liquid layer. The purpose of the paper is to shed light on the proper selection of a bottom plate for an experiment and the necessary correction to the experimental

NOMENCLATURE

a	wavenumber
a_x, a_y	wavenumber in x and y directions
A_0, A, B_0, B	coefficient constants
Bi	Biot number at upper surface, hh_l/k_l
C_1, C_2	integration constants
D	differentiation with respect to z, $\partial/\partial z$
g	gravitational acceleration
h	heat transfer coefficient
h_l, h_s	heights of liquid and solid layers, respectively
k	thermal conductivity
M	Marangoni number defined in equation (9)
n	unit normal vector
p_r, p_i	real and imaginary growth rates with time
Pr	Prandtl number, ν/α
q_0, q	constants defined in equations (29)–(31)
R	Rayleigh number, $g\beta_l\Delta T_l h_l^3/(\alpha_l\nu_l)$
S	surface tension gradient with respect to temperature
T	temperature
w	normal mode component of velocity in z direction
W	eigenfunction of w component
x, y, z	cartesian coordinates.

Greek symbols

α	thermal diffusivity
β	volumetric expansion coefficient
γ	parameter defined in equation (32)
θ	normal mode of temperature perturbation
Θ	eigenfunction of temperature
ν	kinematic viscosity
ρ	density
σ	surface tension.

Subscripts

c	critical value
l	liquid property
r	ratio of liquid property to solid property
s	solid property.

Other symbols

∇^2	Laplacian operator
$(\ )^*$	complex conjugate.

data due to the effect. Since parallel flow assumption has been widely used for the heated-from-below problem [5, 9–14], it is also the purpose of this paper to clarify some features of parallel flow assumptions. In the present analysis the temperatures in the liquid layer and solid plate are expanded in a normal mode form. By requiring the continuity of temperature and heat flux across the interfaces of liquid and solid, and liquid and gas, and by applying necessary conditions on the velocity components, a relation is built to determine the coefficient of the amplitude of the normal mode. The zero determinant of the system leads to the marginal instability. This study shows a qualitatively different feature of boundary effect on the Bénard–Marangoni instability compared to the results previously published.

THEORETICAL ANALYSIS

The experiment setup of Fig. 1 is simplified into a model shown in Fig. 2. Here, the horizontal direction

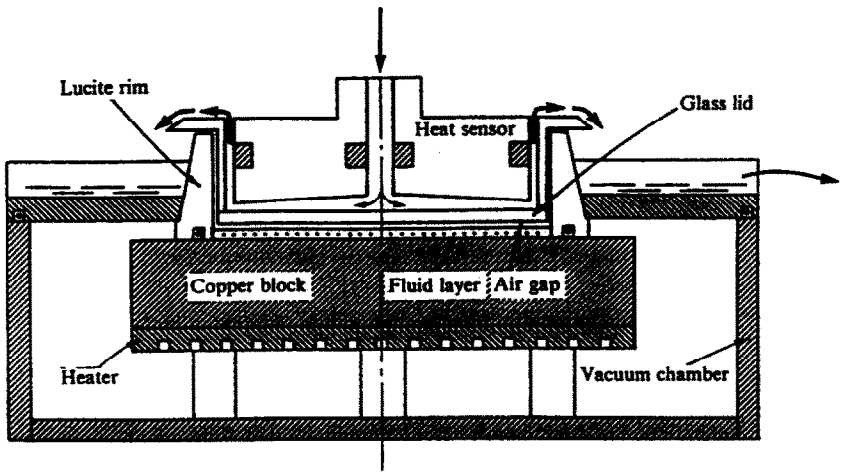

FIG. 1. Experimental schematics.

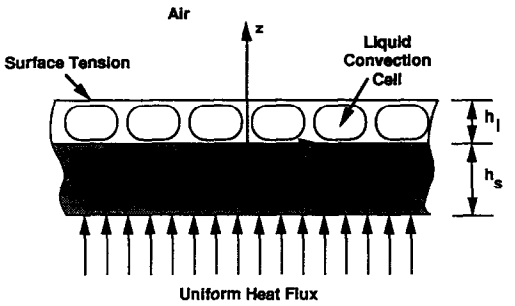

FIG. 2. Mathematical model.

extends to infinity. The solid bottom plate with thickness h_s and thermal conductivity k_s is heated by a uniform heat flux. The horizontal liquid layer with height of h_l has a free upper surface which is in contact with the ambient air. It is postulated that the free surface itself is non-deformable, and surface tension is a linear function of temperature. A cartesian coordinate system is established with g, the gravitational acceleration, in the negative z direction and z is measured from the solid–liquid interface.

Governing equations

Following Chandrasekhar's derivation [15] on the Bénard problem and assuming that the initial quiescent state has a constant temperature gradient $\Delta T_l/h_l$ in the liquid, the dimensionless perturbation equations can be obtained for the liquid as

$$1/Pr\ \partial(\nabla^2 w_l)/\partial t = R(\partial^2\theta_l/\partial x^2+\partial^2\theta_l/\partial y^2)+\nabla^4 w_l \quad (2)$$

$$\partial\theta_l/\partial t = w_l+\nabla^2\theta_l. \quad (3)$$

Here w and θ are the non-dimensional z component of the velocity and the temperature perturbations. Pr and R are the Prandtl number and Rayleigh number, respectively, as defined in the nomenclature. The subscripts l and s represent the quantities in the liquid and solid, respectively, and t represents time. The above equations are obtained on the basis that the physical properties are constant. As usual, ∇^2 is the Laplacian operator

$$\nabla^2 = \partial^2/\partial x^2+\partial^2/\partial y^2+\partial^2/\partial z^2. \quad (4)$$

The non-dimensionalization is made as: velocity by α_l/h_l, time by h_l^2/α_l, temperature by ΔT_l, and length by h_l, where α is the thermal diffusivity.

The perturbation equation for the solid is

$$\partial\theta_s/\partial t = \alpha_s/\alpha_l\nabla^2\theta_s. \quad (5)$$

As for the boundary conditions, the rigid and non-slip conditions for the velocity at solid–liquid interface at $z = 0$ apply

$$w_l = 0, \quad \partial w_l/\partial z = 0 \quad (6)$$

and the continuity of temperature and heat flux requires

$$\theta_l = \theta_s, \quad k_l\,\partial\theta_l/\partial z = k_s\,\partial\theta_s/\partial z \quad (7)$$

with k the thermal conductivity. On the liquid–air interface of $z = 1$, the non-deformation and the balance of shear stress by surface tension gradient lead to

$$w_l = 0, \quad \partial^2 w_l/\partial z^2 = -M(\partial^2\theta_l/\partial x^2+\partial^2\theta_l/\partial y^2) \quad (8)$$

where M is the Marangoni number and is defined as

$$M = S\Delta T_l h_l/(\alpha_l\nu_l\rho_l) \quad (9)$$

$S = -\partial\sigma/\partial\theta$, where σ is surface tension, ν the kinematic viscosity, and ρ the density. The heat exchange of liquid with the ambient air at $z = 1$ can be approximated by

$$\partial\theta_l/\partial z = -Bi\,\theta_l \quad (10)$$

where Bi is Biot number. $Bi = hh_l/k_l$, which is a constant depending on the heat transfer coefficient (h) on the upper surface. The extreme case of $Bi^{-1} = 0$ and $Bi = 0$ are the limiting approximations to very conducting and insulating boundaries.

On the bottom face of $z = -h_s/h_l$, the uniform heat flux applies, so that

$$\partial\theta_s/\partial z = 0. \quad (11)$$

Normal mode

Now we can express the above perturbation quantities in a normal mode form

$$w_l = W_l(z)\exp[i(a_x x+a_y y)+pt] \quad (12)$$

$$\theta_l = \Theta_l(z)\exp[i(a_x x+a_y y)+pt] \quad (13)$$

$$\theta_s = \Theta_s(z)\exp[i(a_x x+a_y y)+pt] \quad (14)$$

where $a = (a_x^2+a_y^2)^{1/2}$ is the wavenumber of the disturbance and p is a complex variable.

$$p = p_r+ip_i \quad (15)$$

p_r is the growth rate of a disturbance with time. If $p_r > 0$, the initial disturbance grows and the initial state is unstable to that disturbance. If $p_r < 0$, the disturbance decays and the initial state is stable. When $p_r = 0$, the initial disturbance is called marginally stable. For a marginally stable disturbance, if p_i is non-zero, a state of fixed amplitude periodic disturbances may exist. If for all marginally stable and amplified disturbances ($p_r \geqslant 0$), p_i is always zero (no oscillatory motion) the normal mode equations can be significantly simplified by setting $p \equiv 0$. This circumstance is commonly referred to as the 'exchange of stability'. Exchange of stabilities has been proven valid for the Rayleigh–Bénard convection subject to a variety of boundary conditions by Pellow and Southwell [16], for Marangoni convection in one fluid layer by Vidal and Acrivos [17], and for a pair of coupled fluid layers by Lienhard [18]. This exchange was postulated without proof by Pearson [19], Scriven and Sternling [20], Nield [1], and Smith [21]. In the analyses of two-layer Bénard–Marangoni instability by Zeren and Reynolds [3] and by Ferm and Wollkind [4], the existence of the exchange of stability has also been assumed. Indeed, if p_i is set at zero and instability

is found, the apparent critical Marangoni number must be an upper bound on the true critical Marangoni number [3]. With due appreciation of this implication, the exchange of stabilities is assumed here and p is set identically zero.

By substituting equations (12)–(14) into equations (2), (3) and (5), we obtain

$$(D^2-a^2)^2 W_1 = R\,a^2\Theta_1 \tag{16}$$

$$(D^2-a^2)\Theta_1 = -W_1 \tag{17}$$

and

$$(D^2-a^2)\Theta_s = 0 \tag{18}$$

with $D = \partial/\partial z$.

The boundary conditions are

at $z = 0$,

$$W_1 = 0, \quad DW_1 = 0 \tag{19}$$

$$\Theta_1 = \Theta_s, \quad k_1 D\Theta_1 = k_s D\Theta_s \tag{20}$$

at $z = 1$,

$$W_1 = 0, \quad D^2 W_1 = M\,a^2\Theta_1 \tag{21}$$

$$D\Theta_1 = -Bi\,\Theta_1 \tag{22}$$

and at $z = -h_s/h_1$

$$D\Theta_s = 0. \tag{23}$$

Solution of eigenfunctions

The eigenfunction of Θ_s can be easily solved from equation (18) as

$$\Theta_s = C_1 \sinh(az) + C_2 \cosh(az) \tag{24}$$

with C_1 and C_2 as integration constants. Let

$$k_r = k_s/k_1, \quad h_r = h_s/h_1. \tag{25}$$

The substitution of the above solution into boundary conditions of (20) and (23) yields a relation for the liquid temperature:

$$D\Theta_1(z=0) = k_r a \tanh(ah_r)\Theta_1(z=0). \tag{26}$$

This is very similar to equation (22), except that Bi is now a function of conductivity ratio k_r, height ratio h_r and wavenumber a. By setting $h_r \to \infty$, the above equation recovers that derived by Lienhard [8], who considered the effect of an infinite thick slab. In Nield's analysis [7], the solid slab is subjected to a uniform temperature condition, and therefore, the above $\tanh(ah_r)$ is replaced by $c\tanh(ah_r)$.

The combination of equations (16) and (17) results in

$$(D^2-a^2)^3 W_1 = -R\,a^2 W_1. \tag{27}$$

The solution of the above equation was first given by Pellow and Southwell [16], and can be found in the book by Chandrasekhar [15]:

$$W_1 = A\cosh(qz) + A^*\cosh(q^*z) + A_0\cos(q_0 z) + B\sinh(qz) + B^*\sinh(q^*z) + B_0\sin(q_0 z) \tag{28}$$

where * denotes a complex conjugate, and A and B are unknown constants. q_0 is a real constant and q is a complex constant, and they depend on Rayleigh number and wavenumber.

$$q_0 = a(\gamma-1)^{1/2} \tag{29}$$

$$\mathrm{Re}\,(q) = a[\tfrac{1}{2}(1+\gamma+\gamma^2)^{1/2} + \tfrac{1}{2}(1+\gamma)]^{1/2} \tag{30}$$

$$\mathrm{Im}\,(q) = a[\tfrac{1}{2}(1+\gamma+\gamma^2)^{1/2} + \tfrac{1}{2}(1+\gamma)]^{1/2} \tag{31}$$

$$R\,a^2 = \gamma^3 a^6, \quad \text{or} \quad \gamma = (R/a^4)^{1/3}. \tag{32}$$

Determination of eigenvalues

Substitution of equation (28) into the appropriate boundary conditions and interface conditions (equations (20)–(22), (26)) yields six linear homogeneous algebraic equations for the six unknown constants A, A^*, A_0, B, B^* and B_0. The non-trivial solution of the system requires the characteristic determinant of the coefficient matrix to vanish. The eigenvalue problem is established as

$$f(R, M, k_r, h_r, Bi, a) = 0 \tag{33}$$

where f is the determinant of the coefficient matrix. With given physical properties of solid and fluid, k_r, h_r, upper surface heat transfer condition Bi, and wavenumber a, we can solve the Rayleigh number R if M is specified, or the Marangoni number M if R is specified. The corresponding critical value of R_c or M_c is determined by a parabolic fit of $R(a)$ or $M(a)$ and by minimizing

$$dR/da = 0 \quad \text{or} \quad dM/da = 0. \tag{34}$$

A computer program was written to calculate the determinant of the matrix by LU decomposition, and Muller's method was used to find the roots of equation (33).

RESULTS AND DISCUSSION

Validation

To validate the present solution, we can compare the predicted wavenumber and critical Rayleigh number with previously published results. For example, by setting $M = 0$, the upper surface is free so that the tabular data from Sparrow *et al.* [22] can be utilized here. In their study, the thermal boundary condition on the upper surface is the same as the present one (equation (22)). They considered the lower surface at the following two limiting conditions: constant temperature and uniform heat flux. These two can be recovered by assigning h_r and k_r to large numbers and by assigning $h_r = 0$, respectively. Under both conditions, we are able to match their wavenumbers exactly, and the critical Rayleigh numbers up to 5th digit at all the upper surface Biot numbers. Another test which can be utilized to make comparison is when the fluid is subjected to a uniform heat flux from below ($h_r = 0$ or $k_r = 0$) and above ($Bi = 0$). Now the critical wavenumber is zero, and it has been shown [5, 23]

that the critical Rayleigh number and the critical Marangoni number are related by

$$R/320 + M/48 = 1. \quad (35)$$

The present calculation is able to fit the above relation exactly.

Rayleigh–Bénard convection

First we consider the case when $M = 0$, which is Rayleigh–Bénard convection with a free upper surface. The critical Rayleigh number, as seen from equation (33), is a function of k_r, h_r and the upper surface Biot number, Bi. Shown in Fig. 3 is the result when the upper surface is kept at a constant temperature, i.e. $Bi^{-1} = 0$. The critical Rayleigh number (R_c) here is presented as a function of the ratio of the solid plate thickness to the liquid layer thickness (h_r) at various values of thermal conductivity ratio (k_r). The two broken lines, taken from ref. [22], corresponds to the critical values when the lower surface of the liquid layer is subjected to a fixed temperature and a fixed heat flux condition. When both k_r and h_r are very small, the constant heat flux supplied by the heating coil to the bottom plate is directly transferred to the liquid layer, and the critical Rayleigh number is close to the asymptotic value of 816.76 given by Sparrow *et al.* [22] for a constant heat flux bottom wall. On the other hand, when both k_r and h_r are high, the bottom plate is equivalent to supplying a constant temperature to the liquid layer and the critical Rayleigh number approaches the value of 1100.66 as from ref. [22]. It is interesting to note that R_c increases with h_r monotonically at the beginning and then approaches a value which depends on k_r. Indeed, h_r comes into play as a boundary condition of equation (26) through function $\tanh(ah_r)$. When h_r is high, the hyperbolic function equals one, so that h_r is dropped out of expression (26) and R_c is independent of h_r.

It is also seen from Fig. 3 that the thermal conductivity ratio (k_r) of the bottom plate to the liquid layer has a significant impact on R_c. For example, when k_r is very low (as low as 10^{-2}), the critical Rayleigh number is almost independent of h_r. The same is also true when k_r is high (such as $k_r = 10^3$). In the typical Rayleigh–Bénard experiment, the liquid layer is very thin so that h_r is in the order of 10^0 to 10^1. It is difficult to provide a 'perfectly insulating' boundary condition for thermal disturbance unless the solid plate is indeed an insulator (k_r is very low). On the other hand, when the plate is made of copper and silicon oil is the working liquid, k_r is in the order of 10^2–10^4. An isotherm condition can be easily fulfilled regardless of the thickness of the solid plate. This explains why most data of Rayleigh–Bénard experiments are for the isothermal boundary condition. The significance of Fig. 3 is that it gives a quantitative criterion to achieve a desirable boundary condition (uniform temperature or constant heat flux).

Figure 3 differs from the Nield's tabular data in that the solid slab in the present study is on the bottom of the liquid, whereas in his case it is on the top. As a result, the critical Rayleigh number in his paper varies from 1295.8 to 1707.8, and for the present case it varies from 816.76 to 1100.66.

The influence of the heat transfer character at the upper free surface on the system stability can be appreciated from Fig. 4, which shows another limiting situation of $Bi = 0$ (Fig. 3 is for $Bi^{-1} = 0$), which corresponds to an insulated upper surface. Again, the broken lines are the asymptotic values for the limiting conditions from ref. [22]. It is seen from the figure that under both limiting perfectly conducting and perfectly insulating conditions on the liquid and solid interface, R_c is dramatically decreased compared to Fig. 3. This is understandable since when the Biot number of the upper surface is zero, any thermal disturbance cannot easily dissipate into the ambience and hence resulting in a reduced R_c. The general trends of R_c dependence on k_r and h_r are the same as that in Fig. 3.

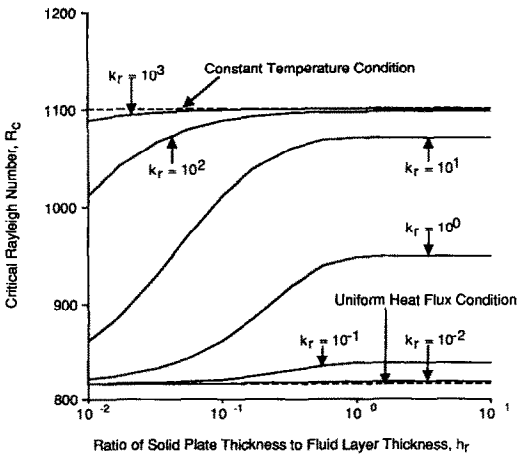

FIG. 3. Critical Rayleigh number for a Rayleigh–Bénard convection with a solid bottom plate and $Bi^{-1} = 0$ at the upper surface.

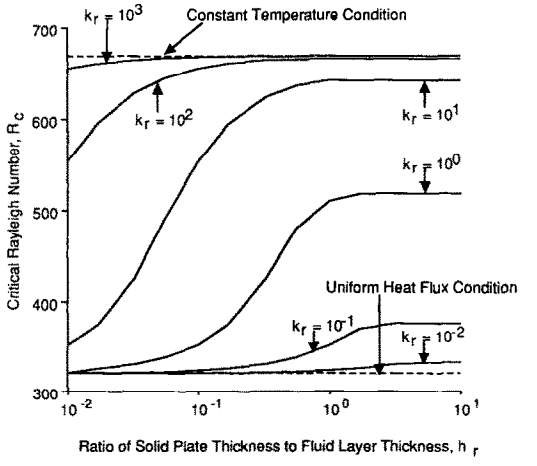

FIG. 4. Critical Rayleigh number for a Rayleigh–Bénard convection with a solid bottom plate and $Bi = 0$ at the upper surface.

Bénard–Marangoni convection

As demonstrated in the last section, for most experiments the role of the solid plate thickness is likely to be minor unless the liquid layer is thick. To this end, we will use $h_r = 10$ in the following calculations.

The (M, R) locus corresponding to marginal stability is plotted in Fig. 5 at several values of thermal conductivity ratios (k_r). The Biot number of the upper surface is 0, so that it is equivalent to insulating the surface. In other words, the heat transfer from the liquid to the ambient air is very poor. The negative Marangoni number in Fig. 5 represents a positive coefficient of surface tension with temperature. For a regularly pure liquid, the surface tension decreases with temperature, resulting in a positive M. When the liquid surface is contaminated by chemical impurity, it is possible that surface tension will reverse its relation with temperature. This gives rise to a negative Marangoni number. The above property of surface tension explains well the 'undercutting' phenomenon observed during welding [24]. First we notice from Fig. 5 that when k_r is small, the bottom plate behaves as an insulator, and the relation of equation (35) is well satisfied. With the increase of the thermal conductivity of the solid plate, the stable region extends. At $k_r = 10^2$ (or even higher), it becomes what has been analyzed by Nield [1]. He gave $R_c = 669.00$ with $a = 2.087$ (when $M = 0$), and our prediction is $R_c = 666.09$ with $a = 2.077$ for $k_r = 10^2$. Figure 5 shows the importance of the selection of the bottom plate in possible suppression of Marangoni convection or Bénard convection.

Under another limit of $Bi^{-1} = 0$, our calculations indicate that the critical Rayleigh number is independent of the Marangoni number. This is because there exists no temperature gradient along the free surface. This has also been predicted by Nield [1]. To study the upper surface heat transfer effect, the (M, R) locus is shown in Fig. 6 for $Bi = 1.0$ and $Bi = 10.0$. From this figure one concludes that a higher heat transfer rate on the upper surface and higher thermal conductivity of the solid plate can all stabilize the fluid layer.

Validity of parallel flow assumption

Parallel flow means that the wavenumber a of a system is zero, so that all the quantities are functions of z with exception of the temperature gradient along the horizontal direction, which is a constant to be determined from the solution. The parallel flow enables a closed-form solution for even very complicated multi-solid–fluid systems [14] or two layer fluid–fluid Bénard–Marangoni system [5]. To make the parallel flow assumption realistic it requires uniform heat flux from the top and the bottom. This may not be easy to achieve in the real experiment, as discussed above, unless k_r or h_r is zero. In this section, we will examine the validity of parallel flow assumption for the present system, i.e. including the conduction of the solid plate which has a finite value of k_r and h_r. We will also examine the possible way to reach the parallel flow condition in experiments.

As shown in the previous section, equation (35) derived for parallel flow can be matched exactly by the present study under a condition of zero value of k_r or h_r and zero value of Biot number on the upper surface. In the following we will set $Bi = 0$, and will study the effect of k_r and h_r on the formation of parallel flow. To obtain a solution of parallel flow for the present system (Fig. 2), let us first review some previous results. When the upper surface is a non-slip wall, it has been shown [5, 14] that the critical Rayleigh number for the liquid and solid system in Fig. 2 is

$$R_c = 720(1 + k_r h_r) \tag{36}$$

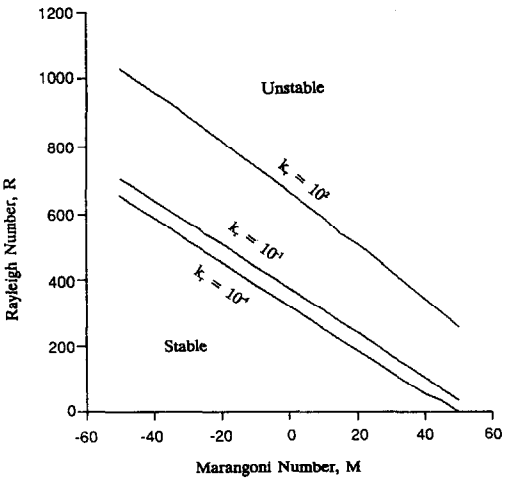

FIG. 5. Locus of Marangoni number and Rayleigh number for $Bi = 0$ at the upper surface.

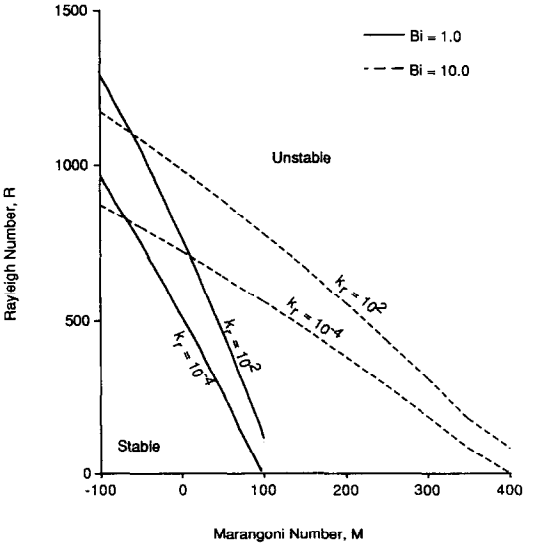

FIG. 6. Locus of Marangoni number and Rayleigh number for $Bi = 1$ and $Bi = 10$ at the upper surface.

where 720 is the critical Rayleigh number for a single fluid layer (no solid plate) [8, 22]. The role of the solid plate is to increase the thermal resistance, thus leading to a more stable system. For the onset motion of the present problem shown in Fig. 2, the parallel flow solution gives (the derivation is omitted here)

$$R/320 + M/48 = 1 + k_r h_r. \tag{37}$$

This relation will be validated by the present study. First it is noticed that $k_r h_r$ is combined as one parameter. According to the boundary condition (26), if a or h_r is small, the expansion of equation (26) on the hyperbolic tangent function gives

$$\tanh(a h_r) \approx a h_r, \quad \text{when} \quad a h_r \to 0 \tag{38}$$

and the thermal boundary condition becomes

$$D\Theta_1 = a^2 k_r h_r \Theta_1 \quad \text{at} \quad z = 0 \tag{39}$$

therefore, it is a function of $k_r h_r$.

Figure 7 gives the critical Rayleigh numbers obtained by the parallel flow solution (equation (37)) and the present solution. The Marangoni number is set to zero, and the independent variable is $k_r h_r$. Several values of h_r are selected. The R_c from parallel flow assumption is linearly dependent on $k_r h_r$. When the height ratio h_r is small, such as $h_r = 10^{-1}$, equation (37) agrees with the present solution up to $k_r h_r = 0.5$. Even when $h_r = 1.0$, the agreement is still favorable up to $k_r h_r = 0.25$. On the other hand, when $h_r = 10^1$, the discrepancy between the two solutions is significant. Apparently, the functional expansion of equation (38) is no longer valid and hence the linear relation of the critical Rayleigh number with $k_r h_r$ does not hold. This shows that the parallel flow assumption is valid only for a small value of h_r. The critical wavenumber corresponding to the curves in Fig. 7 is displayed in Fig. 8. It is noticed that for $h_r = 10^{-1}$ and $h_r = 10^0$, the onset motion is indeed 'parallel' up to $k_r h_r = 0.4$ and 0.18, respectively, and equation (37) is perfect for this range of parameters. Even for finite values of wavenumbers, the critical Rayleigh number calculated from equation (37) is still fairly accurate up to $a = 0.6$ for $h_r = 10^{-1}$ and $h_r = 10^0$. The significance of the finite value of $a = 0.6$ can be appreciated from the fact that in the real system the extension of the horizontal dimension is always finite, and the parallel flow condition can be achieved in an enclosure with an aspect ratio of 0.095 which corresponds to $a = 0.6$.

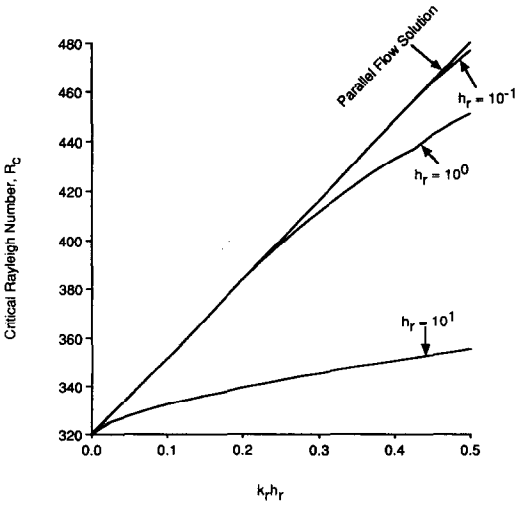

FIG. 7. Comparison of critical Rayleigh numbers from parallel flow solution and the present solution, $Bi = 0$.

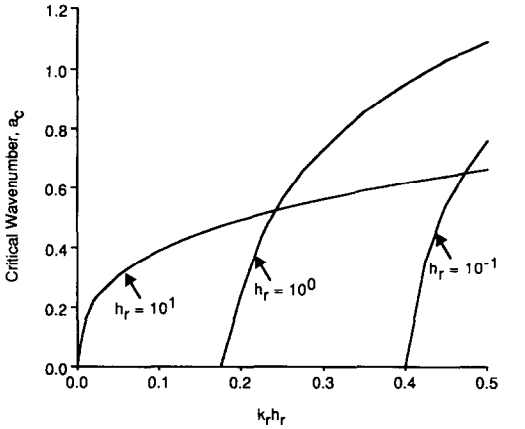

FIG. 8. Critical wavenumber from the present solution, $Bi = 0$.

CONCLUSIONS

An analytical solution is performed to study the characteristics of the stability of a liquid layer which is in contact with a solid plate. The present work distinguishes itself from the previous ones which considered either uniform temperature or uniform heat flux for the Bénard–Marangoni instability. The role of the plate thickness is minor in most of the Bénard–Marangoni experiments, while the conductivity of the plate has a significant impact on the stability of the system. In general, regardless of the upper surface condition, a higher thermal conductivity of the plate leads to a higher critical Rayleigh number. The previous parallel flow analysis is found to be valid when the plate is thin and has a poor conductivity.

REFERENCES

1. D. A. Nield, Surface tension and buoyancy effect in cellular convection, *J. Fluid Mech.* **19**, 341–352 (1964).
2. S. H. Davis and G. M. Homsy, Energy stability theory for free-surface problem: buoyancy-thermocapillary layers, *J. Fluid Mech.* **98**, 527–583 (1980).
3. R. W. Zeren and W. C. Reynolds, Thermal instabilities in two fluid horizontal layers, *J. Fluid Mech.* **53**, 305–327 (1972).
4. E. N. Ferm and D. J. Wollkind, Onset of Rayleigh–

Bénard Marangoni instability: comparison between theory and experiments, *J. Non-Equilib. Thermodyn.* **9**, 169–170 (1982).
5. H. Q. Yang and K. T. Yang, Bénard–Marangoni instability in two-layer system with uniform heat flux, *J. Thermophys. Heat Transfer* **4**, 73–78 (1990).
6. S. H. Davis, Thermocapillary instabilities, *Ann. Rev. Fluid Mech.* **19**, 403–435 (1987).
7. D. A. Nield, The Rayleigh–Jeffreys problem with boundary slab of finite conductivity, *J. Fluid Mech.* **32**, 393–398 (1968).
8. J. H. Lienhard V, An improved approach to conductivity boundary conditions for the Rayleigh–Bénard instability, *J. Heat Transfer* **109**, 378–387 (1987).
9. M. Sen, P. Vasseur and L. Robillard, Parallel flow convection in a tilted two-dimensional porous layer heated from all sides, *Physics Fluids* **31**, 3480–3487 (1988).
10. D. Villers and J. K. Platten, Thermal convection in superposed immiscible liquid layers, *Appl. Sci. Res.* **45**, 145–152 (1988).
11. D. Villers and J. K. Platten, Influence of interfacial tension gradients on thermal convection in two superposed immiscible liquid layers, *Appl. Sci. Res.* **47**, 177–191 (1990).
12. C. H. Wang, M. Sen and P. Vasseur, Analytical investigation of Bénard–Marangoni convection heat transfer in a shallow cavity with two immiscible fluids, *Appl. Sci. Res.* **48**, 35–53 (1991).
13. R. Vasseur, L. Robillard and M. Sen, *Bifurcation Phenomena in Thermal Processes and Convection* (Edited by H. H. Bau, L. A. Bertram and S. A. Korpela), HTD-Vol. 94, pp. 23–30. ASME, New York (1987).
14. H. Q. Yang, Thermal instability and heat transfer in a multi-layer system subjected to uniform heat flux from below, *Int. J. Heat Mass Transfer* **34**, 1707–1715 (1991).
15. S. Chandrasekhar, *Hydrodynamic and Hydromagnetic Stability*. Dover, New York (1961).
16. A. Pellow and R. V. Southwell, On maintained convective motion in a fluid heated from below, *Proc. R. Soc. London A* **176**, 312–343 (1940).
17. A. Vidal and A. Acrivos, Nature of the neutral state in surface tension driven convection, *Physics Fluids* **9**, 615 (1966).
18. J. H. Lienhard V, Thermal instability and heat transfer in a singly partitioned horizontal flow layer, Master's Thesis in Engineering, UCLA (1984).
19. J. R. A. Pearson, On convection cells induced by surface tension, *J. Fluid Mech.* **4**, 489–500 (1958).
20. L. E. Scriven and C. V. Sternling, On cellular convection driven by surface tension gradients: effect of mean surface tension and surface viscosity, *J. Fluid Mech.* **19**, 321–340 (1964).
21. K. A. Smith, On convective instability induced by surface-tension gradients, *J. Fluid Mech.* **24**, 401–414 (1966).
22. E. M. Sparrow, R. J. Goldstein and V. K. Jonsson, Thermal instability in a horizontal fluid layer: effect of boundary conditions and nonlinear temperature, *J. Fluid Mech.* **65**, 209–229 (1974).
23. P. L. Garcia-Ybarra, J. L. Castillo and M. G. Velarde, Bénard–Marangoni convection with a deformable interface and poorly conducting boundaries, *Physics Fluids* **30**, 2655–2661 (1987).
24. H. Q. Yang, A. J. Przekwas and A. C. Nunes, A mathematical model for weld undercutting caused by oxygen contamination, *Welding J.* (submitted).

EFFET DE CONDITION AUX LIMITES SUR L'INSTABILITE DE BENARD–MARANGONI

Résumé—On étudie l'apparition de l'instabilité d'une couche liquide à surface supérieure libre et chauffée en dessous par un enroulement de chauffage à travers une plaque solide. On focalise sur l'effet de la plaque et de sa conductivité. On trouve que cette plaque tend à stabiliser le système si sa conductivité thermique est très élevée. Dans les expériences, il est plus difficile d'obtenir une parfaite condition aux limites d'isolation qu'une parfaite condition de conduction, pour une perturbation thermique. L'hypothèse d'écoulement parallèle est valide quand l'épaisseur de la plaque et sa conductivité thermique sont petites.

RANDEINFLUSS AUF DIE BENARD–MARANGONI INSTABILITÄT

Zusammenfassung—In der vorliegenden Arbeit wird das Einsetzen der Instabilität in einer Flüssigkeitsschicht mit freier oberer Oberfläche untersucht, wobei eine Wärmezufuhr von unten mit Hilfe einer Heizwendel in einer festen Platte stattfindet. Die Arbeit konzentriert sich auf den Einfluß von Dicke und Wärmeleitfähigkeit der Platte. Dabei zeigt sich eine Stabilisierung des Systems bei steigender Wärmeleitfähigkeit. Bei den experimentellen Untersuchungen ist es wesentlich schwieriger eine ideal adiabate Randbedingung zu verwirklichen als eine Randbedingung mit idealer Wärmeleitung. Die Annahme einer Parallelströmung erweist sich für geringe Plattendicke und Wärmeleitfähigkeit als gültig.

ВЛИЯНИЕ ГРАНИЦЫ НА НЕУСТОЙЧИВОСТЬ БЕНАРА–МАРАНГОНИ

Аннотация—Исследуется возникновение неустойчивости жидкого слоя со свободной верхней поверхностью, который нагревается снизу спиралью, проходящей через твердую пластину. Основное внимание уделяется эффекту толщины твердой пластины и ее теплопроводности. Найдено, что пластина с большой теплопроводностью оказывает стабилизирующее воздействие на систему. В натурных экспериментах намного трудней достичь граничное условие с идеальной изоляцией, чем условие с идеальной теплопроводностью для теплового возмущения. Показано, что предположение о параллельном течении справедливо при малых толщине и теплопроводности пластины.